The Astrophysical Journal, 637:L133–L136, 2006 February 1

SPATIALLY RESOLVING THE INNER DISK OF TW HYDRAE

J. A. Eisner,[1,2] E. I. Chiang,[1,3] and L. A. Hillenbrand[4]
Received 2005 December 1; accepted 2005 December 27; published 2006 January 18

ABSTRACT

We present Keck Interferometer observations of TW Hya that spatially resolve its emission at 2 μm wavelength. Analyzing these data together with existing K-band veiling and near-infrared photometric measurements, we conclude that the inner disk consists of optically thin, submicron-sized dust extending from ∼4 AU to within 0.06 AU of the central star. The inner disk edge may be magnetospherically truncated. Even if we account for the presence of gas in the inner disk, these small dust grains have survival times against radiation blowout that are orders of magnitude shorter than the age of the system, suggesting continual replenishment through collisions of larger bodies.

Subject headings: planetary systems: protoplanetary disks — stars: individual (TW Hydrae) — stars: pre–main-sequence

1. INTRODUCTION

TW Hydrae is a nearby (∼51 pc; Mamajek 2005), young (∼10 Myr; Webb et al. 1999) star surrounded by an accretion disk that evinces a large inner hole as judged from the observed spectral energy distribution (SED; Calvet et al. 2002). Unusually low excess emission at wavelengths $\lambda \lesssim 10$ μm can be modeled with an optically thick disk whose inner edge is located ∼4 AU from the central star. While observations of 10 μm silicate emission (Sitko et al. 2000; Uchida et al. 2004) together with nonzero excess at 2 μm (Johns-Krull & Valenti 2001) suggest the presence of at least some dust grains with sizes less than a few microns at stellocentric distances $R \lesssim 4$ AU, this inner disk material appears optically thin and has been estimated to constitute less than a lunar mass (Calvet et al. 2002). Detection of warm gas (Herczeg et al. 2004; Rettig et al. 2004) and accretion signatures (Muzerolle et al. 2000; Alencar & Batalha 2002) confirm that the region inside 4 AU is not devoid of material.

At $R \sim 4$ AU, dust temperatures (∼100 K) are substantially lower than sublimation temperatures for silicate grains ($\gtrsim$1500 K; e.g., Pollack et al. 1994). This suggests that the optically thick outer disk is truncated at 4 AU by a mechanism other than dust sublimation. Large holes inferred from SEDs are commonly attributed to planets, which may clear gaps about their orbits. A planet impedes accretion of material outside its orbit, while inner disk material is free to drain onto the central star (Goldreich & Tremaine 1982; Bryden et al. 1999; Rice et al. 2003). However, a viscous outer disk causes inward migration of planets and their associated gaps (e.g., Lin & Papaloizou 1986; Ward 1997). Thus, inner holes would be filled in on the viscous timescale unless the disk is less massive than the planet, in which case the timescale is lengthened by the mass ratio between the planet and the disk (Chiang 2003). Since the outer disk of TW Hya is massive ($\gtrsim 0.1\ M_\odot$; Weinberger et al. 2002; Wilner et al. 2005), planets are unlikely to preserve inner clearings over the lifetime of the system (∼10 Myr) unless the outer disk is unusually inviscid ($\alpha \lesssim 10^{-5}$; Shakura & Sunyaev 1973).

An alternative explanation for SED-inferred holes is that dust grains have grown larger than a few microns, depleting the population of small grains that would produce the near-IR emission. Scattered light and long-wavelength emission from the outer ($R > 10$ AU) disk of TW Hya suggest substantial grain growth, up to centimeter sizes (Weinberger et al. 2002; Wilner et al. 2005), supporting the hypothesis of grain coagulation. The small amount of submicron-sized dust required to explain emission at $\lambda \lesssim 10$ μm and the spectral shape of the 10 μm silicate feature (Calvet et al. 2002; Uchida et al. 2004) may represent the tail at small sizes of a grain size distribution that peaks at sizes much larger than a micron. Furthermore, as we discuss below, small dust grains are short-lived in the TW Hya disk and demand continual replenishment, possibly from collisions of larger parent bodies. The population of submicron-sized dust in the inner disk may not be primordial.

Here we present observations with the Keck Interferometer that spatially resolve the inner disk around TW Hya for the first time. Previous observations at submillimeter to centimeter wavelengths spatially resolved emission at larger radii (>10 AU) and enabled powerful constraints on the outer disk structure and dust properties (Qi et al. 2004; Wilner et al. 2005). With our near-IR interferometric observations, we extend this analysis to the inner disk. By combining spatially resolved measurements with spectral information, we determine the radial distribution, temperature, and approximate grain sizes of dust. We confirm that the inner disk is populated by small amounts of submicron-sized dust and show that the inner radius[5] of this optically thin disk occurs farther from the star than previous spatially unresolved observations imply.

2. OBSERVATIONS

We observed TW Hya near K-band ($\lambda_K = 2.14$ μm; $\Delta\lambda = 0.3$ μm) with the Keck Interferometer (KI) on 2005 April 21 (UT 20050421). The KI is a fringe-tracking Michelson interferometer that combines light from the two 10 m Keck apertures and provides an angular resolution of $\lesssim$5 mas (Colavita & Wizinowich 2003; Colavita et al. 2003). A single 130 s observation of TW Hya was obtained between observations of three calibrators (HD 97023, HD 97940, and HD 99934). Figure 1 shows the uncalibrated visibilities of the target and calibrators.

[1] University of California at Berkeley, Department of Astronomy, 601 Campbell Hall, Berkeley, CA 94720; jae@astron.berkeley.edu.
[2] Miller Fellow.
[3] Alfred P. Sloan Research Fellow.
[4] California Institute of Technology, Department of Astronomy, Mail Code 105-24, Pasadena, CA 91125.

[5] In the remainder of the Letter, the "inner radius" refers to the inner edge of the optically thin inner disk, not the inner edge of the optically thick outer disk. We take the latter to be located at $R \sim 4$ AU based on previous modeling by Calvet et al. (2002).

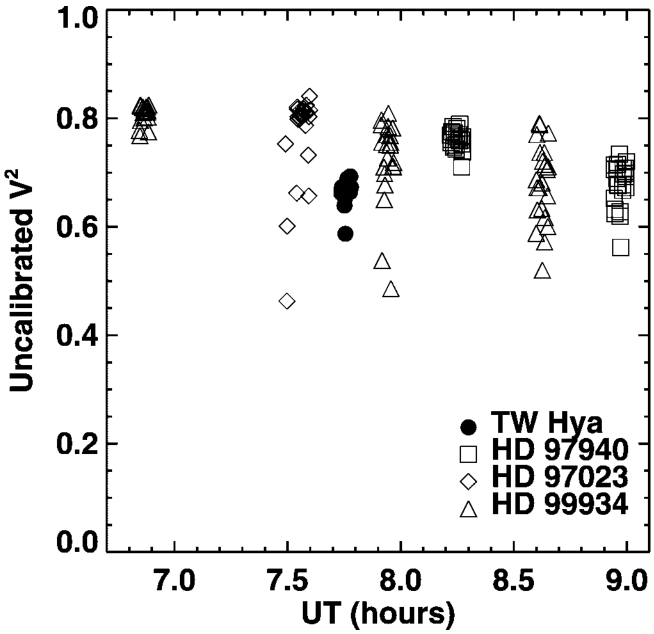

FIG. 1.—Uncalibrated, squared visibilities (V^2) measured by KI for TW Hya and three unresolved calibrator sources. The smaller V^2 value of TW Hya relative to the calibrators indicates that this source is angularly resolved. Scatter in the uncalibrated V^2 is due to a combination of instrumental and atmospheric effects, including variable performance of the Keck adaptive optics systems and phase jitter arising from atmospheric motions and instrumental vibrations.

Data calibration is described by Eisner et al. (2005); here we summarize the procedure. We first determine the system visibility (i.e., the point-source response of the interferometer) from the weighted mean of observations of unresolved calibrators (Boden et al. 1998). Source and calibrator data are corrected for detection biases (Colavita 1999) and integrated into 5 s blocks. The calibrated V^2 for the target source is averaged over all 5 s blocks, with uncertainties given by the quadrature addition of the internal scatter and the uncertainty in the system visibility. The calibrated, normalized, squared visibility measured for TW Hya at $r_{u\text{-}v} = 28$ Mλ ($u = 49.6$ m, $v = 36.7$ m) is $V^2 = 0.88 \pm 0.05$.

3. MODELING

We model our measured V^2 together with previous photometric measurements at $\lambda = 1$–5 μm (Webb et al. 1999; Sitko et al. 2000), assuming photometric uncertainties of 10%. The circumstellar-to-stellar flux ratio is critical for modeling the circumstellar component of the visibility and near-IR SED (e.g., Eisner et al. 2004); we utilize a previous measurement of this ratio at 2 μm, $r_K = 0.07 \pm 0.04$ (Johns-Krull & Valenti 2001). Our model consists of the central star and an optically thin disk. We model the central star using a Kurucz stellar atmosphere with radius $R_* = R_\odot$, temperature $T_* = 4000$ K, mass $M_* = 0.7\ M_\odot$, surface gravity $\log g$ (cm s^{-2}) $= 4.5$,[6] and distance $d = 51$ pc (Webb et al. 1999; Johns-Krull & Valenti 2001; Alencar & Batalha 2002; Mamajek 2005).

The optically thin disk extends from an inner truncation radius $R_{\rm in}$ to an outer radius $R_{\rm out}$. Since most of the near-IR emission is generated close to $R_{\rm in}$ where the hottest dust resides, our results are insensitive to $R_{\rm out}$; for simplicity, we assume $R_{\rm out} = 4$ AU. The mass surface density of the inner disk is parameterized as $\Sigma = \Sigma_0 (R/{\rm AU})^{-3/2}$, where R is the stellocentric radius and Σ_0 is the surface density at $R = 1$ AU.

We assume that dust grains are of a single size and adopt a simple prescription for the frequency-dependent dust opacity, $\kappa_\nu = \kappa_K (\nu/\nu_K)^\beta$ cm^2 g^{-1}. For submicron-sized grains, we set $\beta = 1$ and $\kappa_K = 10^3$. For larger grains with sizes ~10 μm, we take $\beta = 0$ and $\kappa_K = 10^2$. These choices are compatible with previous computations of opacities at $\lambda = 0.1$–5 μm by Miyake & Nakagawa (1993). Our normalizations are ~10^2 times higher than theirs since our κ_ν is the dust-mass opacity as opposed to the dust+gas opacity; i.e., the units of κ_ν are square centimeters per gram of dust.

We compute the dust temperature under the assumption that the disk is optically thin:

$$T_{\rm dust}(R) = T_* \left(\frac{R_*}{2R}\right)^{2/(4+\beta)}. \quad (1)$$

The total flux of the inner disk is derived by dividing the disk into annuli, computing the flux for each annulus, and summing the annular fluxes. Similarly, model visibilities are computed for each annulus, and the visibility for the entire inner disk is given by the flux-weighted sum of the annular visibilities. The flux in an annulus of infinitesimal width dR is

$$dF_\nu(R) = \frac{2\pi}{d^2} B_\nu(T_{\rm dust}) \tau_\nu R\, dR, \quad (2)$$

where B_ν is the Planck function and τ_ν is the vertical optical depth,

$$\tau_\nu(R) = \kappa_\nu \Sigma = \kappa_\nu \Sigma_0 \left(\frac{R}{\rm AU}\right)^{-3/2}. \quad (3)$$

The normalized visibility for an annulus extending from R_1 to $R_2 = R_1 + dR$ is given by the difference of visibilities for uniform disks having radii equal to R_1 and R_2:

$$V(R) = \frac{\lambda d}{2\pi r_{u\text{-}v}(R_2^2 - R_1^2)} \times \left[R_2 J_1\left(\frac{2\pi r_{u\text{-}v} R_2}{\lambda d}\right) - R_1 J_1\left(\frac{2\pi r_{u\text{-}v} R_1}{\lambda d}\right)\right]. \quad (4)$$

Here $r_{u\text{-}v} = 28$ Mλ is the u-v radius, $\lambda = \lambda_K$ is the observing wavelength, and J_1 is a first-order Bessel function.

The total flux density from the disk and the central star equals

$$F_{\nu,\rm tot} = F_{\nu,*} + \int_{R_{\rm in}}^{R_{\rm out}} dF_\nu(R). \quad (5)$$

The veiling at 2 μm is

$$r_K = \frac{1}{F_{K,*}} \int_{R_{\rm in}}^{R_{\rm out}} dF_K(R), \quad (6)$$

where F_K is the flux density at $\lambda = \lambda_K$. The squared visibility of the model at 2 μm is

$$V^2 = \left[\frac{F_{K,*} V_* + \int_{R_{\rm in}}^{R_{\rm out}} dF_K(R) V(R)}{F_{K,\rm tot}}\right]^2, \quad (7)$$

where $V_* = 1$ is the visibility of the unresolved central star.

[6] While the computed $\log g \approx 4.3$ for our assumed values of R_* and M_*, we adopt $\log g = 4.5$ since Kurucz models exist for this value. Our results are insensitive to this small difference.

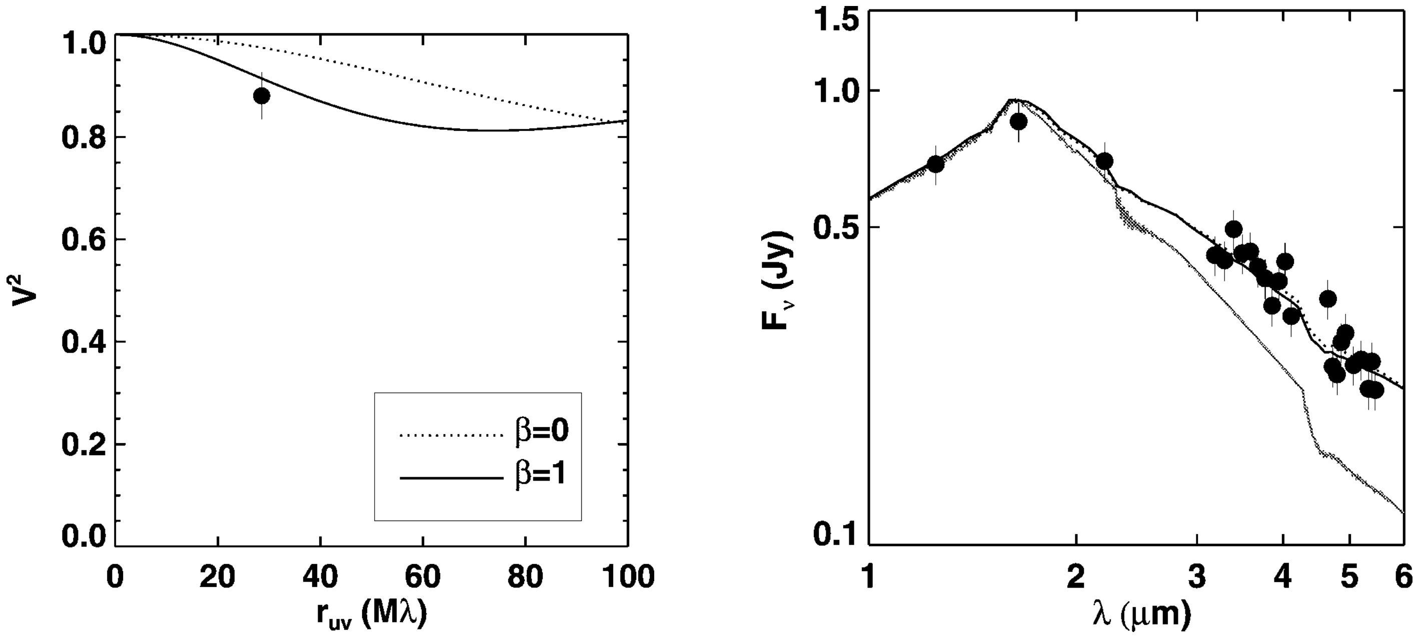

FIG. 2.—Squared visibilities (*left*) and near-IR fluxes (*right*) for a model consisting of a young star surrounded by an optically thin disk, compared to the data (this work; Webb et al. 1999; Sitko et al. 2000). The flux of the central star is indicated by the solid gray line. Models with large dust grains ($\beta = 0$) cannot fit the data well, in contrast to models with submicron-sized dust grains ($\beta = 1$).

We solve for the best-fit parameters of the model by computing the $\lambda = 1$–5 μm fluxes, r_K, and V^2 for a grid of values of $R_{\rm in}$ and Σ_0, and minimizing the χ^2 residuals between model and data. Uncertainties for best-fit parameters are determined from χ^2 error ellipses (e.g., Eisner et al. 2004). We do not include β or κ_K as free parameters and instead consider two model cases: $\beta = 1$ and $\kappa_K = 10^3$ (intended to model submicron-sized grains), and $\beta = 0$ and $\kappa_K = 10^2$ (representing grains sized ~10 μm).

Scattered light from the disk is justifiably ignored in our modeling. At $\lambda = 1.1$ and 1.6 μm, the disk-scattered flux on angular scales of 0″.4–4″ is estimated to comprise 2.4% and 2.1% of the stellar flux, respectively (Weinberger et al. 2002). Given the blue color and roughly flat surface brightness profile of the scattered light within ~0″.8 (Weinberger et al. 2002), we conclude that the *K*-band scattered flux within the 50 mas field of view of KI is <1%. Therefore thermal emission, as traced by the *K*-band veiling (~7% of the stellar flux; Johns-Krull & Valenti 2001), dominates over any scattered emission.

While we have assumed that TW Hya is a single star, a low-mass stellar companion could contribute to the near-IR visibilities and SED. To the best of our knowledge, no stellar companions have been detected in previous *Hubble Space Telescope* imaging or radial velocity monitoring, and thus the presence of a luminous second star appears unlikely. Additional KI observations or astrometric and/or radial velocity monitoring could test this possibility definitively.

4. RESULTS AND DISCUSSION

Figure 2 shows the best-fit models for $\beta = 0$ and 1, together with the V^2 and SED data. Best-fit values for $R_{\rm in}$ and Σ_0 and their 1 σ uncertainties are listed in Table 1. Our model can reproduce the KI V^2 measurement and near-IR SED of TW Hya if $\beta = 1$ and $R_{\rm in} \sim 0.06$ AU. While models with $\beta = 0$ can fit the SED data well (the larger quantity of SED data relative to the single V^2 measurement skews the fits accordingly), only $\beta = 1$ models can simultaneously reproduce our V^2 measurement. From these best-fit parameter values, we compute the temperature at the inner truncation radius $T_{\rm in}$, the dust mass $M_{\rm dust}$,[7] and the 2 μm vertical optical depth at the inner edge $\tau_{K,\,\rm in}$.

The inner radius of the optically thin disk (0.06 AU) exceeds that inferred from previous modeling of spatially unresolved data (0.02 AU; Calvet et al. 2002). Our large inner radius leads to an inner disk temperature lower than expected for dust sublimation (Table 1), suggesting that an alternate truncation mechanism is necessary. One possibility is that the inner disk extends inward to the magnetospheric radius $R_{\rm mag}$, where the ram pressure from accretion balances the stellar magnetic pressure. Although hot dust may still exist interior to this radius, its high

[7] The dust mass depends sensitively on $R_{\rm out}$ and the assumed surface density profile. Estimates of $M_{\rm dust}$ are therefore highly uncertain. For comparison, under the assumption of a constant surface density, Calvet et al. (2002) estimate a dust mass approximately 4 orders of magnitude higher than the values listed in Table 1.

TABLE 1
OPTICALLY THIN DISK MODELS

β	χ_r^2	$R_{\rm in}$ (AU)	$R_{\rm out}$ (AU)	Σ_0 (g cm^{-2})	$T_{\rm in}$ (K)	$M_{\rm dust}$ (g)	$\tau_{K,\,\rm in}$
0	1.17	0.02 ± 0.01	4	$2.0^{+2.0}_{-0.1} \times 10^{-6}$	1400	1×10^{22}	0.07
1	0.98	0.06 ± 0.01	4	$(6.3 \pm 1.5) \times 10^{-7}$	1120	3×10^{21}	0.04

NOTES.—$R_{\rm in}$ is the best-fit inner radius and Σ_0 is the dust surface density at $R = 1$ AU. The outer disk radius $R_{\rm out}$ is fixed for all models. The inner disk temperature $T_{\rm in}$, dust mass $M_{\rm dust}$, and 2 μm vertical optical depth at the inner edge $\tau_{K,\,\rm in}$ are computed for the best-fit values of $R_{\rm in}$ and Σ_0. The value of $M_{\rm dust}$ depends on the assumed surface density profile, $\Sigma \propto R^{-3/2}$; different assumptions regarding this profile yield dust masses that can differ by orders of magnitude.

infall velocity (e.g., Edwards et al. 1994) implies an optical depth orders of magnitude lower than that of dust outside R_{mag}. Assuming an accretion rate of $5 \times 10^{-10}\ M_{\odot}\ \mathrm{yr}^{-1}$ (Muzerolle et al. 2000), a stellar magnetic field strength of 2.6 kG (Yang et al. 2005), and stellar parameters from § 3, we compute $R_{mag} \sim 0.09$ AU (e.g., Königl 1991). This is comparable to our best-fit R_{in} (with $\beta = 1$), indicating that the optically thin inner disk may indeed be magnetospherically truncated.

The fact that models require $\beta = 1$ to fit the combined V^2+SED data indicates that the inner disk contains a population of dust grains having sizes smaller than ∼1 μm. In fact, we can obtain slightly better fits to our data if we allow $\beta > 1$, as one might expect if very small grains ($\lesssim$0.01 μm) were present (Miyake & Nakagawa 1993).

Submicron-sized grains are quickly blown out of the inner disk by stellar radiation pressure. Gas friction mediates dust removal; unbound grains achieve a terminal outflow velocity equal to the product of the momentum stopping time and the net outward acceleration due to radiation pressure and gravity (e.g., Weidenschilling 1977). Estimates of the gas density are necessary to calculate the survival times of small dust grains. Using the measured column density and temperature of H_2 in the inner disk (Herczeg et al. 2004), accounting for the possibility that the midplane may be up to 10^3 times denser than the warm surface (Glassgold et al. 2004; Najita 2006), and assuming a hydrostatic disk, we estimate a midplane gas density[8] at 1 AU of $\lesssim 10^{-15}$ g cm^{-3}. The stopping time for micron-sized grains at $R \sim 1$ AU is $\gtrsim 10^{-2}$ yr, the terminal velocity is $\gtrsim$1 km s^{-1}, and the removal time is $\lesssim$1 yr.

Small dust grains in the TW Hya inner disk survive for $\lesssim$1 yr and are thus ephemeral over the age of the system. Because of the difficulty in transporting submicron-sized grains from the outer disk at $R \gtrsim 4$ AU to $R_{in} = 0.06$ AU, we argue that inner disk dust is continually regenerated, possibly by collisions of a swarm of larger parent bodies that also reside in the inner disk.

[8] Observations of warm CO imply similar gas densities (Rettig et al. 2004; Najita 2006).

5. CONCLUSIONS

We observed TW Hya with the Keck Interferometer and found the 2 μm emission to be spatially resolved. We modeled the interferometric data together with previous measurements of the K-band veiling and near-IR fluxes and inferred that the inner disk consists of optically thin dust extending from the edge of the optically thick outer disk ($R \sim 4$ AU; Calvet et al. 2002) to $R_{in} = 0.06$ AU of the central star. This inner radius is larger than expected from dust sublimation; the truncation may be magnetospheric in origin. The near-IR emitting dust is composed of submicron-sized particles that are extremely short-lived; this dust may be replenished by erosive collisions of larger parent bodies in the inner disk.

The near-IR interferometry data presented in this paper were obtained with the Keck Interferometer (KI) of the W. M. Keck Observatory, which was made possible by the generous financial support of the W. M. Keck Foundation and is operated as a scientific partnership between the California Institute of Technology, the University of California, and NASA. The authors thank the entire KI team for making these observations possible and acknowledge the cultural role and reverence that the summit of Mauna Kea has always had within the indigenous Hawaiian community. The authors are grateful to M. Sitko for providing the 3–5 μm photometry used in this paper and to J. Najita and J. Carr for useful comments about the warm CO gas.

REFERENCES

Alencar, S. H. P., & Batalha, C. 2002, ApJ, 571, 378
Boden, A. F., Colavita, M. M., van Belle, G. T., & Shao, M. 1998, Proc. SPIE, 3350, 872
Bryden, G., Chen, X., Lin, D. N. C., Nelson, R. P., & Papaloizou, J. C. B. 1999, ApJ, 514, 344
Calvet, N., D'Alessio, P., Hartmann, L., Wilner, D., Walsh, A., & Sitko, M. 2002, ApJ, 568, 1008
Chiang, E. I. 2003, ApJ, 584, 465
Colavita, M. M. 1999, PASP, 111, 111
Colavita, M. M., & Wizinowich, P. L. 2003, Proc. SPIE, 4838, 79
Colavita, M. M., et al. 2003, ApJ, 592, L83
Edwards, S., Hartigan, P., Ghandour, L., & Andrulis, C. 1994, AJ, 108, 1056
Eisner, J. A., Hillenbrand, L. A., White, R. J., Akeson, R. L., & Sargent, A. I. 2005, ApJ, 623, 952
Eisner, J. A., Lane, B. F., Hillenbrand, L., Akeson, R., & Sargent, A. 2004, ApJ, 613, 1049
Glassgold, A. E., Najita, J., & Igea, J. 2004, ApJ, 615, 972
Goldreich, P., & Tremaine, S. 1982, ARA&A, 20, 249
Herczeg, G. J., Wood, B. E., Linsky, J. L., Valenti, J. A., & Johns-Krull, C. M. 2004, ApJ, 607, 369
Johns-Krull, C. M., & Valenti, J. A. 2001, ApJ, 561, 1060
Königl, A. 1991, ApJ, 370, L39
Lin, D. N. C., & Papaloizou, J. 1986, ApJ, 309, 846
Mamajek, E. E. 2005, ApJ, 634, 1385
Miyake, K., & Nakagawa, Y. 1993, Icarus, 106, 20
Muzerolle, J., Calvet, N., Briceño, C., Hartmann, L., & Hillenbrand, L. 2000, ApJ, 535, L47
Najita, J. 2006, in IAU Symp. 231, Astrochemistry: Recent Successes and Current Challenges, ed. D. C. Lis, G. A. Blake, & E. Herbst (Cambridge: Cambridge Univ. Press), in press
Pollack, J. B., Hollenbach, D., Beckwith, S., Simonelli, D. P., Roush, T., & Fong, W. 1994, ApJ, 421, 615
Qi, C., et al. 2004, ApJ, 616, L11
Rettig, T. W., Haywood, J., Simon, T., Brittain, S. D., & Gibb, E. 2004, ApJ, 616, L163
Rice, W. K. M., Wood, K., Armitage, P. J., Whitney, B. A., & Bjorkman, J. E. 2003, MNRAS, 342, 79
Shakura, N. I., & Sunyaev, R. A. 1973, A&A, 24, 337
Sitko, M. L., Lynch, D. K., & Russell, R. W. 2000, AJ, 120, 2609
Uchida, K. I., et al. 2004, ApJS, 154, 439
Ward, W. R. 1997, ApJ, 482, L211
Webb, R. A., Zuckerman, B., Platais, I., Patience, J., White, R. J., Schwartz, M. J., & McCarthy, C. 1999, ApJ, 512, L63
Weidenschilling, S. J. 1977, MNRAS, 180, 57
Weinberger, A. J., et al. 2002, ApJ, 566, 409
Wilner, D. J., D'Alessio, P., Calvet, N., Claussen, M. J., & Hartmann, L. 2005, ApJ, 626, L109
Yang, H., Johns-Krull, C. M., & Valenti, J. A. 2005, ApJ, 635, 466